Medical Dosimetry, Vol. 27, No. 1, pp. 37–42, 2002

0958-3947/02/$–see front matter

PII: S0958-3947(02)00086-9

DOSIMETRIC CHARACTERISTICS WITH SPATIAL FRACTIONATION USING ELECTRON GRID THERAPY

A. S. MEIGOONI, S. A. PARKER,[1] J. ZHENG,[2] K. J. KALBAUGH,[3] W. F. REGINE, and M. MOHIUDDIN

University of Kentucky, Chandler Medical Center, Department of Radiation Medicine, Lexington, KY

(*Received* 30 *July* 2001; *Accepted* 11 *November* 2001)

Abstract—Recently, promising clinical results have been shown in the delivery of palliative treatments using megavoltage photon grid therapy. However, the use of megavoltage photon grid therapy is limited in the treatment of bulky superficial lesions where critical radiosensitive anatomical structures are present beyond tumor volumes. As a result, spatially fractionated electron grid therapy was investigated in this project. Dose distributions of 1.4-cm-thick cerrobend grid blocks were experimentally determined for electron beams ranging from 6 to 20 MeV. These blocks were designed and fabricated at out institution to fit into a 20 × 20-cm^2 electron cone of a commercially available linear accelerator. Beam profiles and percentage depth dose (PDD) curves were measured in Solid Water phantom material using radiographic film, LiF TLD, and ionometric techniques. Open-field PDD curves were compared with those of single holes grid with diameters of 1.5, 2.0, 2.5, 3.0, and 3.5 cm to find the optimum diameter. A 2.5-cm hole diameter was found to be the optimal size for all electron energies between 6 and 20 MeV. The results indicate peak-to-valley ratios decrease with depth and the largest ratio is found at D_{max}. Also, the TLD measurements show that the dose under the blocked regions of the grid ranged from 9.7% to 39% of the dose beneath the grid holes, depending on the measurement location and beam energy. © 2002 American Association of Medical Dosimetrists.

Key Words: **Spatial fractionation, Grid, Electron therapy.**

INTRODUCTION

The use of grid or spatial fractionation in radiotherapy is described in the literature as far back as the early 1900s.[1,2] Early grid radiotherapy involved placing a wire mesh grid directly on the patient's skin.[1,2] In the 1960s, during the Orthovoltage era, grids were used to increase skin tolerance for the treatment of bulky tumors requiring large irradiation fields.[3] In an animal model study, Urano *et al.*[4] found that with grid therapy, the tolerance of skin, soft tissue, and tumors increased by a factor of 1.8, 1.8, and 1.23, respectively, leading to a gain of 1.5. However, the implementation of skin-sparing megavoltage photon radiotherapy decreased the need for spatial fractionation.

In 1960, Mauderli *et al.*[5] described the dosimetric properties of grid Cobalt-60 teletherapy as a function of grid hole diameter and spacing. The results of this study revealed that the dose under the blocked areas relative to the dose under the grid holes decreased as grid hole diameter decreased and as spacing between grid holes increased. Miller *et al.*[6] have investigated the effect of a grid on whole-body irradiation on C3Hf/SED mice using Cobalt 60 teletherapy unit. They found an increase of $LD_{50/30}$ by a factor of 1.5 for mice receiving grid irradiation. Recently, megavoltage photon grid therapy has been utilized in palliative therapy, and promising clinical results have been achieved.[7,8] However, the use of megavoltage photon grid therapy is of limited used in the treatment of superficial lesions where critical radiosensitive structures are present beyond tumor volumes and in the exit path of the photon beams.

Electron grid radiotherapy may overcome these limitations of photon grid therapy. In a synopsis of grid radiation therapy, Loevinger[3] cited several sources describing electron grid therapy with electron beams of 6 to 35 MeV that were published in the 1950s and 1960s.[9,10] The majority of the sources were published in the early days of x-ray research and therefore are not easily accessible. Moreover, no recent research involving the application of modern technology for electron grid therapy was found in the literature and it is not clear why this modality has been discontinued. Given our experience and recent success with photon grid therapy,[7–8,11–12] we have decided to investigate the application of electron grid therapy (EGT) in treatment of bulky superficial tumors where underlying critical structures are of poten-

Reprint requests to: Ali S. Meigooni, Ph.D., DABR, Department of Radiation Medicine, Chandler Medical Center, 800 Rose Street, University of Kentucky, Lexington, KY 40536. E-mail: alimeig@pop.uky.edu

[1]Present Address: Forsythe Regional Cancer Center, Department of Radiation Oncology, 3333 Silas Creek Parkway, Winston-Salem, NC 27103.

[2]Present Address: Radiation Oncology of Las Vegas, Suite 100, 3006 S. Maryland Pkwy., Las Vegas, NV 89109.

[3]Present Address: Robert Boissoneault Cancer Institute, 2020 SE 17th Street, Ocala, FL 34471.

This project was presented at the 1998 AAPM Annual Meeting in San Antonio, TX.

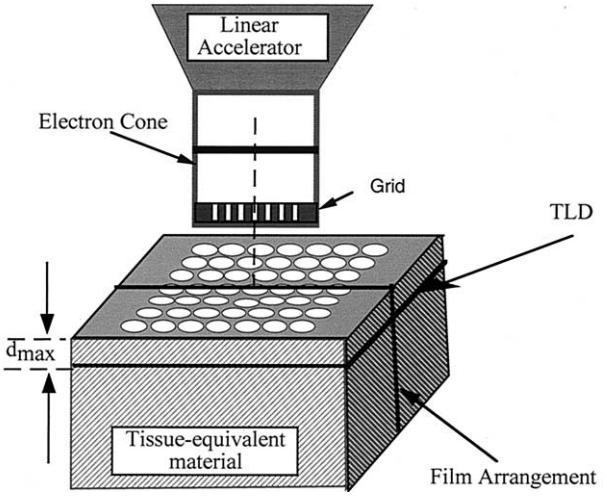

Fig. 1. Schematic diagram of the experimental setup for film and TLD dosimetry in Solid Water phantom. Films were aligned parallel to the beam central axis. TLDs were placed at D_{max}.

tial concern, and therefore may prohibit the use of photon grid therapy (PGT).

In this study, dosimetric characteristics (*i.e.*, percentage depth dose and beam profiles) of the 6- to 20-MeV electron-grid beams are determined experimentally. Also, the variation of dose distribution as a function of grid hole diameter is evaluated.

MATERIALS AND METHODS

Dose distributions of electron grids were studied using 6-, 9-, 12-, 16- and 20-MeV electron beams from a Varian Clinac 2100C/D linear accelerator (Varian Associates, Palo Alto, CA). The 1.4-cm-thick cerrobend grid blocks were designed and fabricated at our institution to fit into the 20 × 20-cm^2 electron cone of the linear accelerator. Dose measurements were performed in Solid Water phantom material (Radiation Measurements Inc., RMI, Middleton, WI) using Kodak XV-2 silver halide radiographic film (Eastman Kodak Company, Rochester, NY) and LiF TLD (TLD-100, Harshaw, Solon, OH). Figure 1 shows the schematic diagram of the experimental setup.

The initial block was designed to have 0.9-cm-diameter holes spaced at 1.5-cm intervals. The percentage depth dose curve of this grid (Fig. 2) indicated that we could only treat to a depth of 2 cm with 80% isodose line using 20-MeV electron beam. This was felt to be clinically suboptimal. Therefore, it was decided to search for an optimal grid hole diameter that is able to treat to a reasonable depth while benefiting from spatial fractionation of the beam (Fig. 3). This grid has a minimal scatter contribution from adjacent grid holes. Two films were exposed for each electron energy and scanned with a WP 102 Wellhöfer densitometer (Wellhöfer Dosimetrie, Schwarzenbruck, Germany) to obtain the percent depth

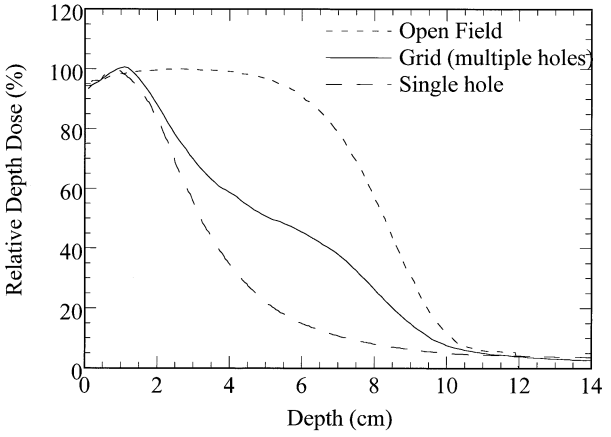

Fig. 2. Comparison of the percent depth dose of an open field for 20-MeV electron beam with that of single and multiple grid hole blocks. The hole diameter of the grid block was 0.9 cm.

dose curve for each grid hole. The results were compared with the open-field data to obtain the optimum diameter. The optimum diameter was defined here as a size that would provide a treatment radiation dose (*i.e.*, 80% of D_{max}) to a depth of approximately 50% of an open-field radiation.

The results displayed clinically suboptimal differences in the penetration characteristics of the electron beams with grid hole diameters less than 2.5 cm (Fig. 4). Moreover, diameters greater than 2.5 cm limited the number of holes in the treatment area (while not significantly increasing the PDD characteristics) and hence were also suboptimal for spatially fractionated treatment. Therefore, a 2.5-cm hole diameter was found to be an

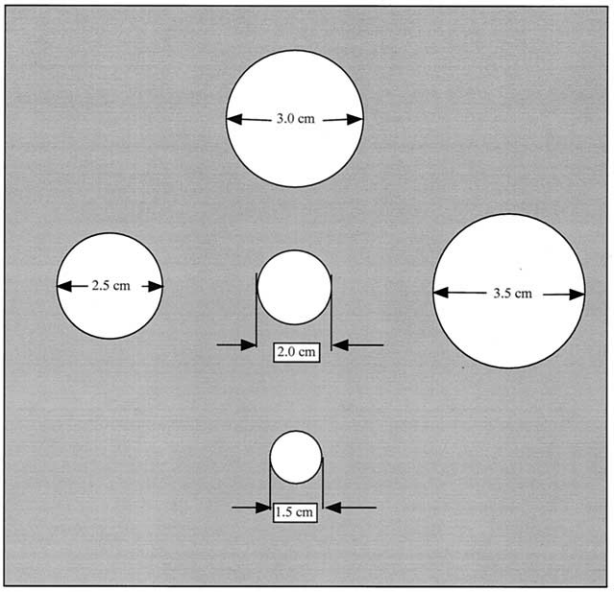

Fig. 3. Schematic diagram of a grid block with various diameter holes. This grid was used to determine the optimal grid hole diameter.

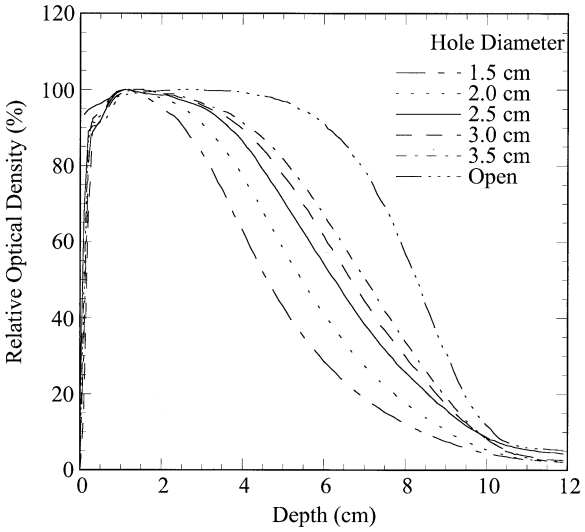

Fig. 4. Relative optical density curves as a function of the grid hole sizes compared with open field data.

optimal hole size for all electron energies between 6 and 20 MeV. Thus, a 5 × 5 matrix of 2.5-cm-diameter holes spaced every 3.0 cm was manufactured (Fig. 5). This resulted in a clinical treatment area of 14.5 × 14.5 cm^2 with approximately 40% of the area blocked. At least 2 films were exposed for each electron energy and both grids, as described previously. Also, films were exposed under calibration conditions (SSD = 100 cm, cone size = 20 × 20 cm^2, depth of maximum dose) at varying doses to allow conversion from optical density to dose. Figure 6 shows a sample of the films exposed to a 20-MeV electron beam using the 0.9-cm diameter hole grid. Similar films were obtained for the 2.5-cm-diameter hole grid for each electron energy.

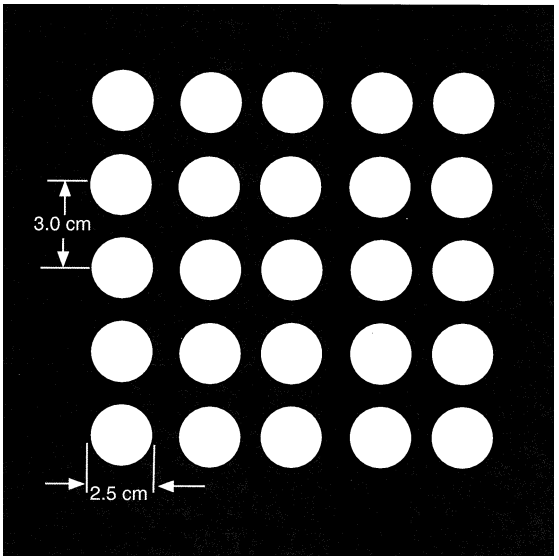

Fig. 5. Schematic diagram of the grid block with 2.5-cm-diameter holes. The grid holes were spaced at 3 cm center-to-center intervals.

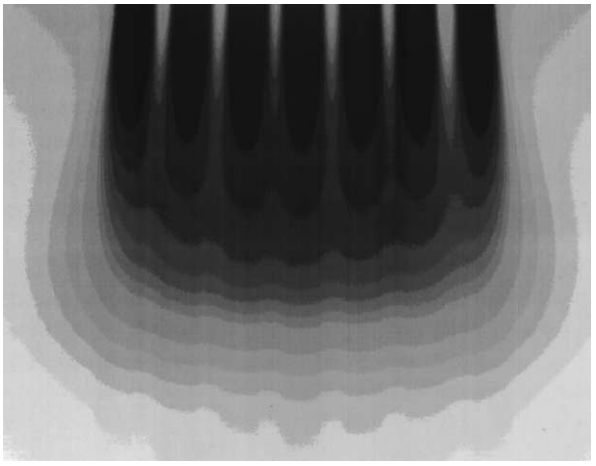

Fig. 6. A sample film exposed with the 0.9-cm-diameter hole grid using 20-MeV electron beam.

Beam profiles and percentage depth dose curves were measured for the 0.9- and 2.5-cm diameter multihole grids using 6-, 9-, 12-, 16-, and 20-MeV electron beams. Percentage depth dose curves were also measured for the single hole grids. These measurements were performed along the central axis of the beam, which coincides with the longitudinal axis of the central hole. Dose distribution in the buildup region, at D_{max}, and at least one depth beyond D_{max} were measured with a PTW N233343 Markus-type parallel plate chamber (PTW).

TLD measurements were obtained at D_{max} with the 2.5-cm-diameter multihole grid for each electron energy (Fig. 1). The absolute doses at the center of the open areas (under grid holes) and under shielded areas between 2 and 4 grid holes were measured using TLD chips (TLD-100, 3 × 3 × 0.9 mm^3). At least 4 TLD chips were placed at each measurement location and the measurements were repeated in order to obtain results with ±3%

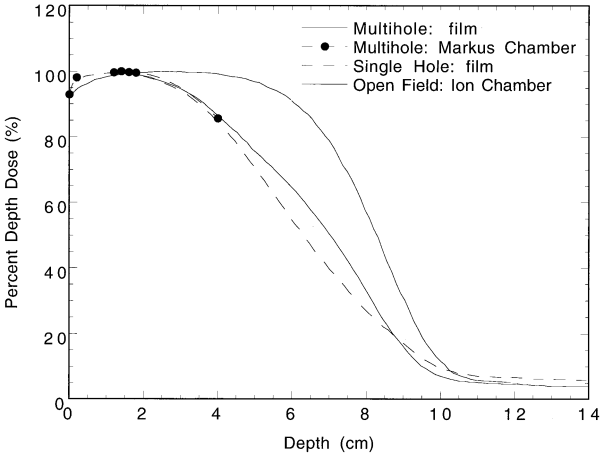

Fig. 7. 20-MeV electron percentage depth dose cures obtained using the 2.5-cm-diameter hole grid, a 2.5-cm-diameter single-hole block, and an open beam. The solid circles are measured data using a Markus-type parallel plate ionization chamber.

Table 1. Comparison of depth of maximum dose in an open field with that of a grid filed with 2.5-cm diameter holes, as a function of electron beam energy

Electron beam energy (MeV)	Depth of maximum dose (mm)	
	Open field	Grid field
6	13	9
9	22	11
12	30	14
16	35	16
20	28	14

precision. TLDs were calibrated for each electron beam energy under calibration conditions (SSD = 100 cm, cone size = 20 × 20 cm^2, depth of maximum dose). TLDs were read with a Harshaw TLD reader (Models 2000A and 2000B, Harshaw Nuclear System, Solon, OH). The TLD readings were converted to absolute dose.

RESULTS

Percentage depth doses of 6-, 9-, 12-, 16-, and 20-MeV electrons were measured using film and ionization chambers. Figure 7 shows the percentage depth dose curves of 20 MeV measured with 2.5-cm-diameter hole grid, a 2.5-cm diameter single hole block, and an open field. Similar results were obtained for other electron beams.

From the PDD curves, we have determined the depth of maximum dose in the grid field. Table 1 shows a comparison of the depth of maximum dose between the open field and grid field as a function of energy. This table indicates that the depths of maximum dose for 6-, 9-12-, 16-, and 20-MeV electron beams in a grid field were 9, 11, 14, 16, and 14 mm, respectively. However, in an open field, the depths of maximum doses for the above energies were 13, 22, 30, 35, and 28 mm, respectively. To eliminate any possible confusion between these 2 sets of values, the depths of maximum doses in a grid field will be referred to as the grid depth of maximum dose. For clinical applications of the grid fields, we have also measured the depths of 90% and 80% dose, as shown in Table 2.

Table 3 shows the output factor (cGy/MU) of the electron grid field measured at the grid depths of maximum dose (Table 1, 3rd column) for each electron beam energy as compared to the machine output in an open field. Table 4 presents the values of the absolute and relative doses at the center of the holes and between the holes of the grid blocks as measured with LiF TLD at 100-cm SSD. These results indicate that the dose under the block between 2 adjacent holes falls between 22.7% and 39% of the dose in the center of a grid hole, at the depth of maximum dose. However, the dose between 4 adjacent holes were found to range from 9.4% to 11.9% of the dose in the center of a grid hole, at grid depth of maximum dose. These values were also measured at 105 and 110 cm SSD for 6 and 20 MeV, as shown in Table 5.

Figure 8 shows beam profiles for a 20-MeV electron grid beam at depths of 14 (D_{max}), 30, 40, and 50 mm. The profiles are normalized to the central axis dose value at the grid depth of maximum dose. As shown in this figure, peak-to-valley dose ratios decrease with depth and the maximum ratio is at the grid depth of maximum dose. Tissue at 5-cm depth will receive an average of 70% of the maximum dose. Moreover, tissue under blocked regions at the grid depth of maximum dose, will receive about 30% of the maximum dose. Similarly, dose

Table 2. Depths of 100%, 90%, and 80% dose for each electron energy in 2.5-cm diameter grid holes radiation field using 100-cm SSD

Electron beam energy (MeV)	Depth of grid electron beams (mm)		
	100%	90%	80%
6	9	15.5	18.0
9	11	21.5	25.5
12	14	26.0	32.0
16	16	30.0	37.5
20	14	36.0	46.0

Table 3. Output factor (cGy/MU) of the electron grid (2.5-cm holes) field measured at the depth of maximum dose for a 20 × 20-cm electron applicator as compared to an open field

Electron beam energy (MeV)	Output factor (cGy/MU)	
	Grid field	Open field
6	0.817	1.000
9	0.936	1.000
12	0.951	1.000
16	1.011	1.000
20	1.065	1.000

For an open field radiation, the machine output was calibrated to be 1.0 cGy/MU at the depth of maximum dose (see second column of Table 1) using a 20 × 20-cm electron applicator, and 100-cm SSD.

Table 4. Measured dose rates at the center of 2.5-cm diameter grid holes and shadow of the grid blocks as a function of electron energy

Electron beam energy	Dose measured at:					
	Center of holes		Under block between 2 holes		Under block between 4 holes	
MeV	(cGy)	%	(cGy)	%	(cGy)	%
6	81.7	100	32.0	39.0	7.9	9.7
9	93.6	100	31.7	33.9	8.8	9.4
12	95.1	100	26.6	28.0	9.4	9.9
16	101.1	100	23.0	22.7	11.2	11.1
20	106.5	100	28.7	26.9	12.7	11.9

These measurements were performed at 100-cm SSD using the maximum field of irradiation by the grid block.

Table 5. Measured doses at the center of grid holes and shadow of the grid blocks as a function of electron beam energy and SSD for 2.5-cm diameter grid hole size

SSD (cm)	Electron beam energy (MeV)	Dose measured at: Center of the holes (cGy)	Center of the holes (%)	Shadow (cGy)	Shadow (%)
100	6	81.7	100	7.9	9.7
100	20	106.4	100	12.7	11.9
105	6	71.5	100	22.5	31.4
105	20	92.2	100	12.5	13.5
110	6	55.7	100	31.7	56.9
110	20	82.8	100	16.6	20.1

profiles for the 12-MeV electron grid beams at depths of 14, 20, 30, and 40 mm are shown in Fig. 9. With this electron energy, tissue at 4-cm depth receives an average of 65% of the dose.

DISCUSSIONS AND CONCLUSIONS

Design, fabrication, and dosimetric characterization of an electron grid block have been described here for treatment of bulky superficial tumors. A 1.4-cm-thick cerrobend electron grid block was fabricated to fit into the electron cone of the Varian 2100 C/D linear accelerator. The grid hole size was investigated to find an optimum dimension that would provide a penetration depth of approximately 50% of an open field (at 80% dose level) in the tissue. The ratio of the open/blocked area for this grid block was 60%/40%. Relative dose distribution and absolute doses for 6-, 9-, 12-, 16-, and 20-MeV electron beam energies were measured in Solid

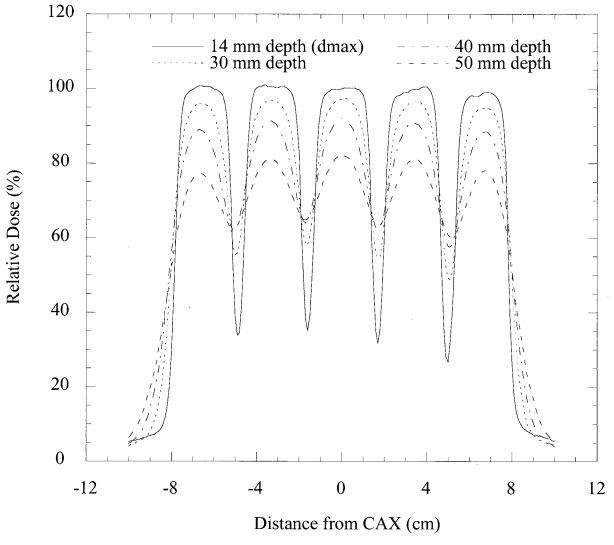

Fig. 8. Beam profiles for 20-MeV spatially fractionated electron beams using the 2.5-cm diameter hole grid at depths of 14 (D_{max}), 30, 40, and 50 mm.

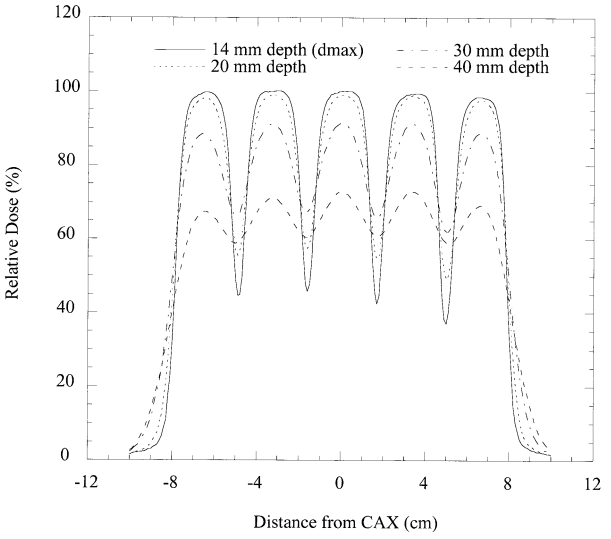

Fig. 9. Beam profiles for 12-MeV spatially fractionated electron beams using the 2.5-cm diameter hole grid at depths of 14 (D_{max}), 20, 30, and 40 mm.

Water phantom using XV-2 radiographic film and LiF TLD.

The results of these investigations show that the depths of maximum dose for 6-, 9-, 12-, 16-, and 20-MeV electron beams were reduced from 13, 22, 30, 35, and 28 mm, respectively, in an open field to 9, 11, 14, 16, and 14 mm, respectively, in a grid field. These results are in agreement with the published data that the depth of maximum dose shifts toward the surface as the field size reduces. Also, for clinical applications of the grid blocks, depths of 90% and 80% doses were measured (Table 2).

The output factors (cGy/MU) of the electron beams with a grid block were measured at the grid depths of maximum dose for all of the beam energies (Tables 3 and 5). Also, doses to the shadow of the block relative to the center of the holes indicate that the dose under the block, between 4 adjacent holes, was approximately 9% to 12% of the dose in the center of a grid hole, at grid depth of maximum dose. Ratio of the peak-dose to valley-dose was changing as a function of depth, with their maximum value being at grid depth of maximum dose.

In summary, a 2.5-cm hole diameter grid block was found to be optimal for electron therapy in the energy range of 6 to 20 MeV. Dosimetric characteristics of the electron grid were measured for its clinical applications. A biological study is being conducted to find the clinical advantages of electron grid therapy.

REFERENCES

1. Köhler, H. “Theorie einer Methode bisher unmöglich anwendbar hohe Dosen Röntgenstrahlen in der Tiefe von Geweben zur therapeutischen Wirksamkeit zu bringen ohne schwere Schädigung des Patienten, zugleich eine Methode des Schutzes gegen Röntgenverbrennung überhaupt,” *Fortschr. A. d. Geb. D. Röntgenstrahlen* **14:**27–9; 1909.

2. Köhler, H. Zur Röntgentiefentherapie mit Massendosen, *Med. Wochenschr.* **56:**2314–6; 1909.
3. Loevinger, R. Grid therapy, physical part. In: Encyclopedia of Medical Radiology Berlin: Springer-Verlag; 1970:461–94.
4. Urano, M.; Kaneda, G.; Shimazaki, S.; *et al.* Radiation dose tumor-control assays for irradation through a sieve. *Am. J. Roentgenol.* **102:**38–42; 1968.
5. Mauderli, W.; Gould, D.M.; Lane, J.W. Focussed grid telecobalt film dosimetry. *Am. J. Roentgenol.* **83:**514–9; 1960.
6. Miller, R.C.; Wilson, K.G.; Feola, J.M. Megavoltage grid total body irradiation of C3Hf/SED mice. *Strahlenther. Onkol.* **168:** 423–6; 1992.
7. Mohiuddin, M.; Curtis, D.L.; Grizos, W.T.; *et al.* Palliative treatment of advanced cancer using multiple nonconfluent pencil beam radiation: A pilot study. *Cancer* **66:**114–8; 1990.
8. Mohiuddin, M.; Stevens, J.H.; Reiff, J.E.; *et al.* Spatially fractionated (GRID) radiation for palliative treatment of advanced cancer. *Radiat. Oncol. Invest.* **4:**41–7; 1996.
9. Ovadia, J.; Duplex, J.; McIsaac, D. Treatment planning with electrons of 20–35 MeV for deep-seated tumors. *Radiology* **72:**99–100; 1959.
10. Ovaida, J.; McAllister, J. Dose distribution in grid therapy with 15 to 35 MeV electrons. *Radiology* **76:**118–9; 1961.
11. Ahmed, M.A.; Meigooni, A.S.; Fruitwala, S.M.; *et al.* Spatially fractionated (GRID) radiation: TNF-mediated therapeutic gain in enhanced cell killing of radioresistant tumor cells. *Radiat. Res. Oncol.* Submitted.
12. Mohiuddin, M.; Fujita, M.; Regine, W.F. High-dose spatially-fractionated radiation (GRID): A new paradigm in the management of advanced cancers. *Int. J. Radiat. Oncol. Biol. Phys.* **45:**721–7; 1999.